DC-Arcing Detection by Noise Measurement With Magnetic Sensing by TMR Sensors

Wenchao Miao, Xuyang Liu, K. H. Lam, and Philip W. T. Pong

Department of Electrical and Electronic Engineering, The University of Hong Kong, Hong Kong

An arc fault establishes a current path in the air which may cause malfunction of direct current (dc) system and even a fire hazard. Arc fault detection is essential to improving the reliability, efficiency, and safety of the dc system. However, the randomness of dc arc faults makes it difficult to define their characteristics. In this paper, a magnetic-sensing-based technique is proposed to detect dc arc. This paper developed a promising dc-arcing detection technique based on the analysis of frequency-domain features of the magnetic field measured by a magnetic sensor. The effects of the supply voltage, load current, and electrode diameter on the frequency domain of the arc current were investigated. The experimental results show that the proposed detection technique could reliably discriminate the normal operation and arc fault. This technique is cost-effective because it can be implemented with low-cost magnetoresistive sensors and does not require an expensive current transformer.

Index Terms—**Direct current (dc) arc fault, fault detection, magnetoresistive sensor, noise measurement.**

I. Introduction

DIRECT current (dc) systems have received increasing attention with the development of renewable energies, electrical vehicles, storage devices, and other applications involving dc [1]–[5]. DC arc fault, which is unintentional and harmful, challenges the safety, reliability, and efficiency of the dc system. It may be caused by aged or damaged wires, a loose connection of connectors, and the accidental current path between conductors. The undetected arc faults may spread to adjacent circuits and even lead to fire hazards. For example, dc arc faults in photovoltaic (PV) systems have already caused several fire hazards worldwide [6]. According to National Electrical Code 2011, arc fault protection is required for PV systems with a maximum voltage larger than 80 V. In order to detect the dc arc faults, various detection techniques have been widely researched.

There are mainly three methodologies to detect dc arc faults: frequency-spectrum analysis, wavelet transformation, and electromagnetic radiation. The wavelet transformation attains the arc information in a time–frequency domain for arc detection, but the accuracy depends on the correct selection of the "mother wavelet" [7], [8]. The electromagnetic radiation of dc arc from 1 to 100 MHz could be used for arc detection [9], [10]. However, the appearance and amplitude of the arc signals are arbitrary leading to the difficulty and unreliability in identifying dc arc. Although the frequency-spectrum analysis detecting arc through the signatures of the frequency domain is of higher accuracy and is widely adopted [11]–[13], the aimed frequency range and the threshold of power spectra to differentiate between dc arc and normal operation are unspecific. Despite the fact that different methodologies have been researched to detect dc arc faults, the characteristics of dc arc need further investigation and reliable techniques to detect dc arc faults are still lacking.

In this paper, the proposed technique can detect dc arc by the analysis of frequency-domain features of the arc current measured by a magnetoresistive sensor. A model composing of pink noise and white noise is introduced to analyze the frequency spectra of the arc current. The fitting parameters of the model can be used to effectively identify dc arcing. Magnetoresistive sensors are capable of measuring electric current [14], and they are of low cost and small volume. Hence, this technique can be cost-effective and compact.

In Section II, an experimental system was developed to study the characteristics of dc arc. The performance of the magnetoresistive sensor was examined by comparing the measurement results with that obtained with a current probe. In Section III, the influence of supply voltage, load current, and electrode diameter on the frequency domain of the arc current were investigated. The frequency spectra of arc current were numerically fit by the pink noise equation. The derived parameters were used to distinguish the normal operation and sustained arcing. The conclusion is drawn in Section IV.

II. Arc Detection System Based on Magnetic Sensing

A. Experimental Setup

The experimental setup consists of an arc generator, resistive loads, a 10 kW dc power supply, a current probe, a tunnel magnetoresistance (TMR) sensor (MultiDimension TMR2001), amplifiers, and an oscilloscope. Fig. 1(a) and (b) shows the photograph of the setup. The dc power supply, arc generator, and resistive load were connected in series. The dc arc was induced between the two copper electrodes by operating the stepper motor to create a gap length of 0.5 mm. The current probe and TMR sensor were used to measure the load current in normal operation and sustained arcing. The TMR sensor senses the current based on the magnetoresistance effect of a magnetic tunnel junction (MTJ). The electrical resistance of

Manuscript received March 16, 2018; revised April 29, 2018; accepted May 26, 2018. Date of publication June 25, 2018; date of current version October 17, 2018. Corresponding author: P. W. T. Pong (e-mail: ppong@eee.hku.hk).

Color versions of one or more of the figures in this paper are available online at http://ieeexplore.ieee.org.

Digital Object Identifier 10.1109/TMAG.2018.2842187

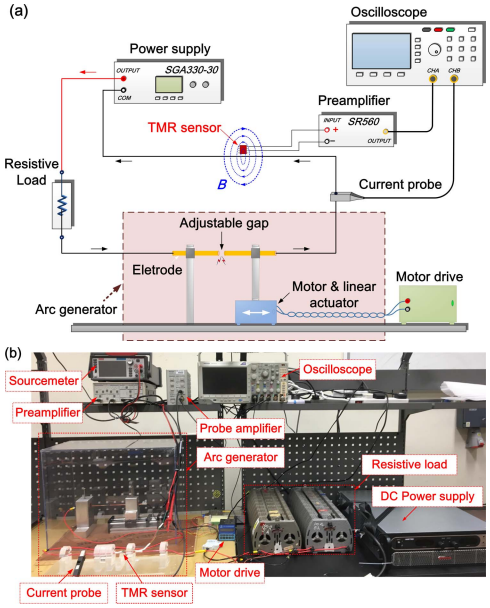

Fig. 1. Experimental setup of the arc detection system. (a) Diagram of the setup. (b) Photograph of the setup.

TABLE I
EXPERIMENTAL CONDITION

Electrode material	Copper
Electrode diameter (mm)	3, 5
Gap length (mm)	0.5
Supply voltage (V)	48 to 300 in step of 12
Load current (A)	4, 5, 6, 8, 10, 16

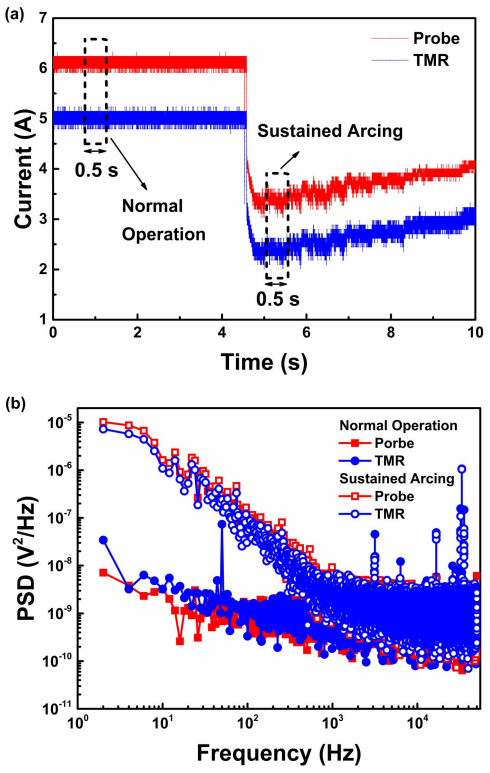

Fig. 2. Current from the TMR sensor and current probe when supplied with 48 V and 6 A. (a) Time-domain current waveforms (the current measured by the TMR sensor is shifted downward by 1 A for clarity). (b) PSD from 2 Hz to 50 kHz.

an MTJ changes as a function of the magnetic field emanated from the current, and thus the current can be determined based on this phenomenon [15]. The TMR2001 exhibits a typical TMR ratio around 200%, and it can provide high sensitivity of 80 mV/V/mT [16]. It was supplied with a constant voltage of 5 V and operated within its linear range of the transfer curve. The experimental conditions are provided in Table I. The characteristics of arcing were investigated from 48 to 300 V in a step of 12 V. The experiments of different current and electrode diameters were also conducted to evaluate their influences on dc arc.

B. Background and Methodologies

The load current was measured by the current probe and TMR sensor in the experiment with the 3 mm diameter of copper when supplied with 48 V and 6 A. As shown in Fig. 2, from a period of 0.5 s of their time-domain current waveforms [Fig. 2(a)], the frequency spectra [Fig. 2(b)] of normal operation current and sustained arcing current were extracted, respectively. The measurement results in Fig. 2(a) suggest that the current in normal operation and sustained arcing can be measured by both the TMR sensor and the current probe. Although the arc current detected by TMR sensor was larger in oscillations, the magnitude and variations were consistent with the results from the current probe. Therefore, the fast Fourier transform (FFT) spectra of the current waveform measured from the TMR sensor and the current probe are similar to those depicted in Fig. 2(b).

In the presence of an arc fault, the frequency spectrum of the load current is composed of both pink and white noises [17]–[19]. The significant increase of the power spectral density (PSD) at low-frequency range from 0 to 1 kHz as shown in Fig. 2(b) can be attributed to the pink noise. Equation (1) can be applied to numerically fit the frequency spectra by a superposition of pink and white noises characterized by the fitting parameters of slope (γ) and magnitude (A). These fitting parameters can then be used to determine the presence of the dc arc

$$S(f) = \frac{A}{f^{\gamma}} + c \tag{1}$$

where S is the PSD, f is the frequency, and A, γ, and c are constants.

The current probes and current transformers (CTs) used in current research are bulky and expensive which can easily cost over several hundred dollars [7], [17], [20]. The TMR2001 only costs a few dollars, and the size is about 3 mm × 3 mm × 1.5 mm. Therefore, the size of sensor is largely reduced by over 100 times and a cost reduction by over 90%, comparing with the relatively low-cost CT [17], can be achieved with this technique. More importantly, the TMR sensing approach is superior to the current probe approach because it is non-contact and it does not require making contact and clamping around the cable.

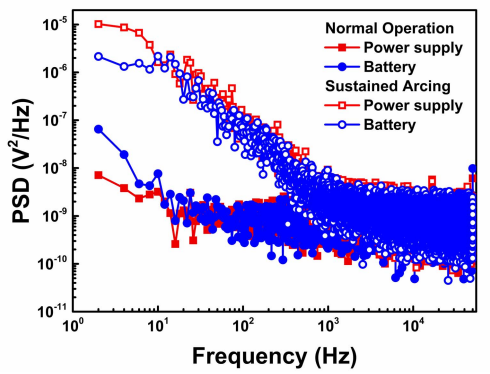

Fig. 3. Frequency spectra of the current when supplied with the power supply and the batteries.

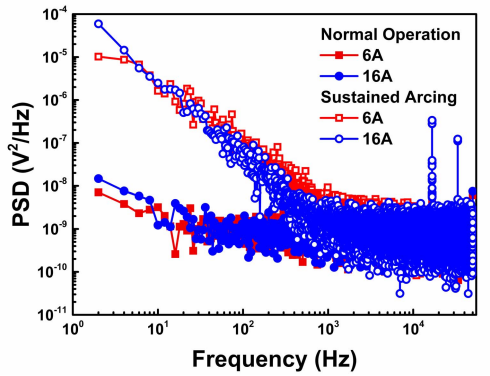

Fig. 4. Frequency spectra of the current at 6 and 16 A when supplied with 48 V.

III. Analysis of Frequency-Domain Features

A. Source of the Pink Noise

In order to verify that the pink noise was not caused by the power source, the experimental results obtained with dc power supply were compared with that obtained with batteries. Four 12-V lead-acid batteries were connected in series to provide 48 V. According to Fig. 3, their frequency spectra of the arc current are similar to those obtained with the dc power supply which indicates that the pink noise did not come from the power source. Since the resistive load does not produce pink noise [21], [22], the only possible source of the pink noise is the dc arc.

B. Effects of Current and Electrode Diameter on Arcing

The experiments with a supply voltage of 48 V and the load current varied from 6 to 16 A were carried out to investigate the current effect on the frequency-domain features of the dc arc. As shown in Fig. 4, the frequency-spectrum PSD of the load current at 16 and 6 A are similar.

The electrodes of the diameter of 3 and 5 mm were used in the experiments at 48 V and 300 V with a load current of 6 A to investigate its effect on the characteristic of dc arc. The frequency spectra under normal operation and sustained arcing are shown in Fig. 5. The spectra of electrode diameter of 3 and 5 mm are similar except the strength of the pink noise at low frequency decreased slightly with the electrode diameter from 3 to 5 mm. In summary, the effects of load-current magnitude and electrode diameter on the strength of the pink noise of the arc current are insignificant, although the effects could be stronger for larger current or electrode diameter.

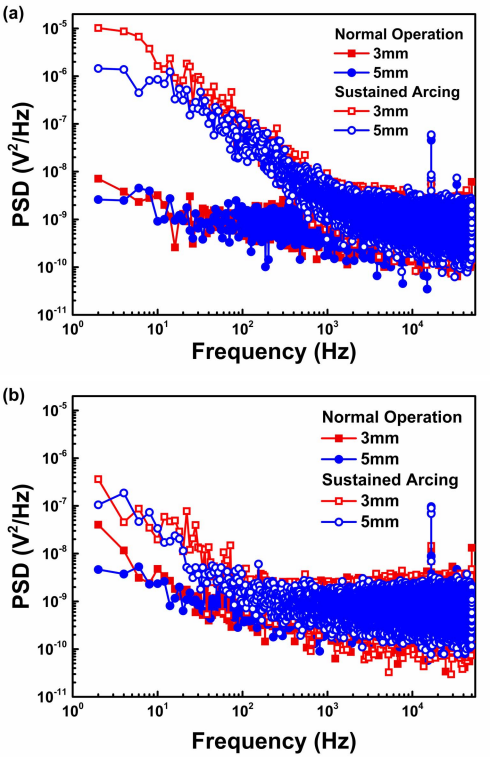

Fig. 5. Frequency spectra of the current with electrode diameter in 3 and 5 mm when supplied with (a) 48 and (b) 300 V.

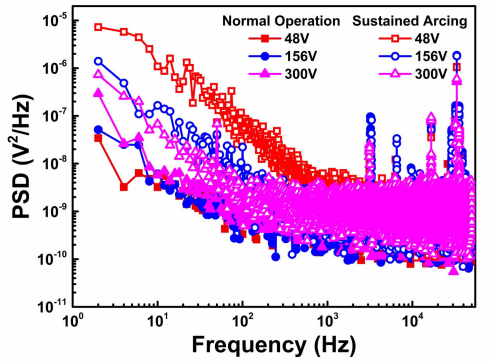

Fig. 6. FFT spectra of normal operation and sustained arcing at 48, 156, and 300 V, respectively.

C. Effects of Voltage on Arcing

In order to study the voltage effect on dc arc, experiments were conducted with the voltage increased from 48 to 300 V in a step of 12 V. The experiments were carried out at a load current of 6 A with the 3 mm diameter of copper electrodes. The presence of arc caused a significant increase of the PSD from 0 to 1 kHz which could be attributed to

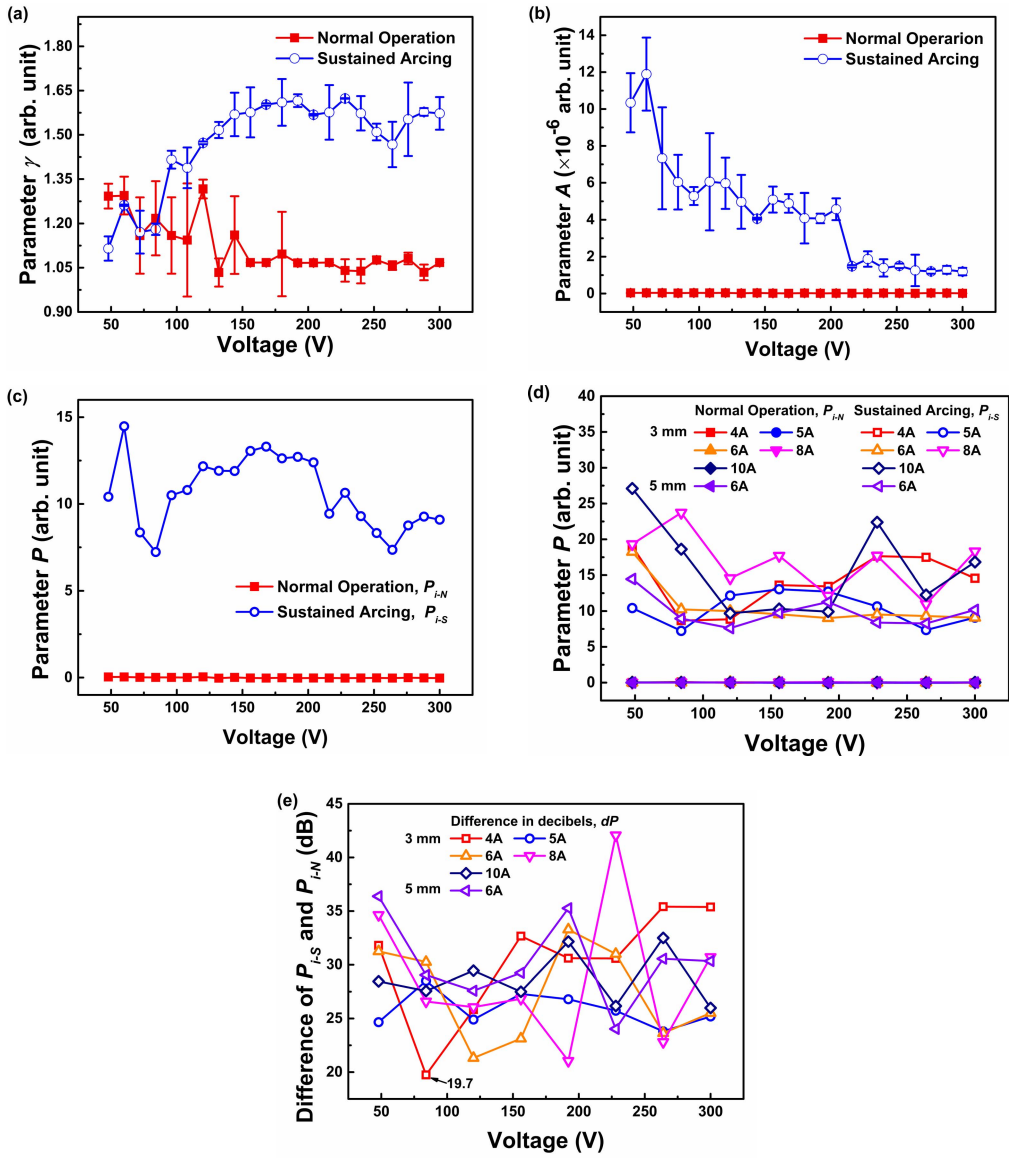

Fig. 7. Fitting results of normal operation and sustained arcing from 48 to 300 V. (a) Fitting results of γ at 5 A. (b) Results of A at 5 A. (c) Combined parameter P at 5 A and an electrode diameter of 3 mm. (d) Parameter P at 4, 5, 6, 8, and 10 A for an electrode diameter of 3 mm and 6 A for 5 mm. (e) Difference between P_{i-S} and P_{i-N} in decibels.

the pink noise as explained in Section II. This phenomenon was particularly pronounced for the arcing at a lower voltage (e.g., 48 V). As the voltage increases, the arc current becomes more similar in nature to the normal operation current. Therefore, the strength of the pink noise of the arc current decreased with the voltage. This trend is clearly demonstrated by the results measured by the TMR sensor at 48, 156, and 300 V in Fig. 6.

D. Methodology to Identify Arcing

In order to identify the dc arc, the pink noise induced by arcing from 48 to 300 V was investigated. The frequency spectra of the arc current were fit by (1), and the fitting results of γ and A were extracted. The fitting results at 5 A and electrode diameter of 3 mm are shown in Fig. 7(a) and (b). The parameter differences between normal operation and arcing can be applied to determine the presence of dc arc. However, there is no discrepancy in γ for voltage lower than 120 V and A for voltage over 228 V. Therefore, it is necessary to combine γ and A to achieve a parameter that can be applied for identification of arc throughout the whole voltage range from 48 to 300 V.

Since γ increases, while A decreases with the voltage, the combination of them should be close to a flat curve with the clear discrepancy between normal operation and arcing. The combined parameter P is derived from γ and A using (2). γ is scaled by k, which is the mean value of γ divided by A as the scale factor, to make γ and A in the same order of magnitude. The combined parameter P is the summation of scaled γ and A. The combined parameter P shows clear discrepancy between normal operation (P_{i-N}) and sustained

arcing (P_{i-S}) throughout the whole voltage range from 48 to 300 V, as depicted in Fig. 7(c)

$$P_i(P_{i-N}, P_{i-S}) = \left[\left(\frac{\gamma_i}{k} - \gamma_1\right) \times 10 + A_i\right] \times 10^6$$
$$k = \frac{\sum_{i=1}^{N} \frac{\gamma_i}{A_i}}{N}$$
$$i = 1, 2, 3, \ldots 22 \quad \text{(denotes the voltage from 48 V to 300 V in step of 12 V)} \quad (2)$$
$$dP = 10 \log \left| \frac{P_{i-S}}{P_{i-N}} \right| \quad (3)$$

where P_i is the combined parameter, P_{i-N} is the P_i in normal operation, P_{i-S} is the P_i in sustained arcing, γ_i is the γ from 48 to 300 V, γ_1 is the γ at 48 V, k is the mean value of (γ_i/A_i), and dP is the difference between P_{i-S} and P_{i-N} in decibels.

The combined parameter P for the normal operation and sustained arcing at 4, 6, 8, and 10 A from 48 to 300 V in a step of 36 V with an electrode diameter of 3 mm and at 6 A with an electrode diameter of 5 mm was derived and compared. These results are shown in Fig. 7(d). The difference between P_{i-N} and P_{i-S} in decibels can be calculated from (3), and the results are shown in Fig. 7(e). According to Fig. 7(d) and (e), the combined parameter P shows clear discrepancy (with a difference of at least 19.7 dB) between P_{i-N} and P_{i-S} under all these situations with different voltages, currents, and electrode diameters. This is consistent with the findings that the effects of current and electrode diameter on frequency-domain features of dc arcing are insignificant.

Consequently, this arc detection technique was demonstrated to be capable of identifying arc using the combined parameter P under various voltage, current, and electrode diameter.

IV. Conclusion

The effects of voltage, current, and electrode diameter on dc arc were studied by analyzing the frequency-domain features of arc current measured by a TMR sensor. The pink noise generated by arcing was evaluated to derive the parameter for reliable identification of arc. The effectiveness of the proposed technique was demonstrated for dc-arcing detection from 48 to 300 V and current up to 16 A. The technique was also applicable with different electrode diameters (3 and 5 mm, respectively). A clear discrepancy of over 19.7 dB was observed between normal operation and sustained arcing with this technique. Future work will be focused on further investigating the effects of voltage, current, and electrode diameter beyond the range studied in this paper to more precisely determine the working region of this detection technique.

Acknowledgment

This work was supported in part by the Seed Funding Program for Basic Research, the Seed Funding Program for Applied Research, and the Small Project Funding Program from The University of Hong Kong, Hong Kong, in part by the ITF Tier 3 Funding under Grant ITS/203/14, Grant ITS/104/13, and Grant ITS/214/14, in part by RGC-GRF under Grant HKU 17204617, and in part by the University Grants Committee of Hong Kong under Contract AoE/P-04/08.

References

[1] J. M. Carrasco *et al.*, "Power-electronic systems for the grid integration of renewable energy sources: A survey," *IEEE Trans. Ind. Electron.*, vol. 53, no. 4, pp. 1002–1016, Jun. 2006.

[2] Z. Q. Zhu and D. Howe, "Electrical machines and drives for electric, hybrid, and fuel cell vehicles," *Proc. IEEE*, vol. 95, no. 4, pp. 746–765, Apr. 2007.

[3] M. Yilmaz and P. T. Krein, "Review of battery charger topologies, charging power levels, and infrastructure for plug-in electric and hybrid vehicles," *IEEE Trans. Power Electron.*, vol. 28, no. 5, pp. 2151–2169, May 2013.

[4] S. Vazquez, S. M. Lukic, E. Galvan, L. G. Franquelo, and J. M. Carrasco, "Energy storage systems for transport and grid applications," *IEEE Trans. Ind. Electron.*, vol. 57, no. 12, pp. 3881–3895, Dec. 2010.

[5] D. Salomonsson and A. Sannino, "Low-voltage DC distribution system for commercial power systems with sensitive electronic loads," *IEEE Trans. Power Del.*, vol. 22, no. 3, pp. 1620–1627, Jul. 2007.

[6] H. Haeberlin and M. Real, "Arc detector for remote detection of dangerous arcs on the DC side of PV plants," in *Proc. 22nd Eur. Photovoltaic Solar Energy Conf.*, Milan, Italy, 2007, pp. 1–26.

[7] X. Yao, L. Herrera, S. Ji, K. Zou, and J. Wang, "Characteristic study and time-domain discrete- wavelet-transform based hybrid detection of series DC arc faults," *IEEE Trans. Power Electron.*, vol. 29, no. 6, pp. 3103–3115, Jun. 2014.

[8] Z. Wang and R. S. Balog, "Arc fault and flash signal analysis in DC distribution systems using wavelet transformation," *IEEE Trans. Smart Grid*, vol. 6, no. 4, pp. 1955–1963, Jul. 2015.

[9] C. J. Kim, "Electromagnetic radiation behavior of low-voltage arcing Fault," *IEEE Trans. Power Del.*, vol. 24, no. 1, pp. 416–423, Jan. 2009.

[10] Q. Xiong, S. Ji, L. Zhu, L. Zhong, and Y. Liu, "A novel DC arc fault detection method based on electromagnetic radiation signal," *IEEE Trans. Plasma Sci.*, vol. 45, no. 3, pp. 472–478, Mar. 2017.

[11] Texas Instruments, Dallas, TX, USA. (2012). *AN-2154 RD-195 DC Arc Detection Evaluation Board*. Accessed: Apr. 3, 2018. [Online]. Available: http://www.ti.com/lit/ug/snoa564f/snoa564f.pdf

[12] S. McCalmont, "Low cost arc fault detection and protection for PV systems: January 30, 2012–September 30, 2013," Nat. Renew. Energy Lab., Golden, CO, USA, Tech. Rep., 2013.

[13] S. Chae, J. Park, and S. Oh, "Series DC arc fault detection algorithm for DC microgrids using relative magnitude comparison," *IEEE J. Emerg. Sel. Topics Power Electron.*, vol. 4, no. 4, pp. 1270–1278, Dec. 2016.

[14] C. Reig, M.-D. Cubells-Beltrán, and D. R. Muñoz, "Magnetic field sensors based on giant magnetoresistance (GMR) technology: Applications in electrical current sensing," *Sensors*, vol. 9, no. 10, pp. 7919–7942, Oct. 2009.

[15] J. Lenz and A. S. Edelstein, "Magnetic sensors and their applications," *IEEE Sensors J.*, vol. 6, no. 3, pp. 631–649, Jun. 2006.

[16] MultiDimension. *TMR2001*. Accessed: Apr. 30, 2018. [Online]. Available: http://www.dowaytech.com/en/index.php?c=download&id=2025

[17] M. Wendl, M. Weiss, and F. Berger, "HF characterization of low current DC arcs at alterable conditions," in *Proc. 27th Int. Conf. Electr. Contacts (ICEC)*, Jun. 2014, pp. 1–6.

[18] F. Schimpf and L. E. Norum, "Recognition of electric arcing in the DC-wiring of photovoltaic systems," in *Proc. 31st Int. Telecommun. Energy Conf. (INTELEC)*, Oct. 2009, pp. 1–6.

[19] J. Keenan and M. Parker, "Arc detectors," in *Proc. 20th Int. Telecommun. Energy Conf. (INTELEC)*, Oct. 1998, pp. 710–715.

[20] J. Johnson *et al.*, "Differentiating series and parallel photovoltaic arc-faults," in *Proc. 38th IEEE Photovoltaic Spec. Conf. (PVSC)*, Jun. 2012, pp. 000720–000726.

[21] J. Pierce, "Physical sources of noise," *Proc. IRE*, vol. 44, no. 5, pp. 601–608, May 1956.

[22] F. N. Hooge, "1/f noise sources," *IEEE Trans. Electron Devices*, vol. 41, no. 11, pp. 1926–1935, Nov. 1994.